Evaluation of directionality in physics-based ground motion simulations of strike-slip earthquakes

Nathan Girmay,[a)] M.EERI, Alan Poulos,[a)] M.EERI, Eduardo Miranda[a)] M.EERI

Recent advances in engineering seismology and computing power have led to the development of realistic physics-based ground motion simulations. The use of these simulations for engineering applications requires that the ground motions exhibit characteristics consistent with those of recorded ground motions. While several studies have evaluated the intensity, frequency content, duration, and other characteristics of ground motion simulations for their possible use in engineering applications, few have focused on directionality. This paper evaluates directionality in the response of single-degree-of-freedom oscillators when subjected to CyberShake Study 15.12 simulated ground motions from strike-slip earthquakes, by carefully comparing it to the directionality in recorded ground motions having the same style of faulting. Physics-based ground motion simulations at 334 stations from 5 different rupture variations in two large-magnitude earthquake scenarios on the Elsinore fault are evaluated. The orientation of maximum oscillator response and its spatial distribution are studied for each rupture. The orientation of maximum oscillator response is found to occur systematically close to the epicentral transverse orientation at all rupture distances, consistent with recent findings for ground motions recorded during strike-slip earthquakes. Additionally, the orientation-specific spectral accelerations, when computed as a function of angular distance from the epicentral transverse orientation, are found to exhibit a variation consistent with the overall trend observed in records from the NGA-West2 database. However, the level of polarization at short periods in the simulated hybrid broadband waveforms used in this study is larger than that in recorded ground motions.

INTRODUCTION

[a)] Department of Civil and Environmental Engineering, Stanford University, Stanford, CA, USA
Corresponding author: Nathan Girmay, Department of Civil & Environmental Engineering, Stanford University, 473 Via Ortega, Stanford, CA, 94305, USA
Email: ngirmay3@stanford.edu

Advances in seismology and computational power in the past few decades have led to the development of sophisticated physics-based ground motion simulations (e.g., Graves and Pitarka, 2010; Mai et al., 2010). Current design codes in the United States (ASCE, American Society of Civil Engineers, 2022) permit the use of physics-based ground motions as possible inputs for nonlinear response history analyses in the absence of suitable recorded ground motions. Using simulated ground motions is especially beneficial for sites located at short distances from the rupture during large-magnitude earthquakes, where only a relatively small number of records are currently available. The adoption of simulated ground motions for engineering use, however, is only appropriate if they can adequately reproduce the main characteristics of recorded ground motions. In the past decade, there have been numerous efforts to validate simulated ground motions for engineering applications (e.g., Bijelić et al., 2018; Burks et al., 2015; Burks and Baker, 2014; Fayaz et al., 2020; Galasso et al., 2020; Teng and Baker, 2019). It is widely recognized that the intensity of ground motions recorded during past earthquakes, typically characterized by 5%-damped response spectral ordinates, can greatly vary with changes in horizontal orientation at a given site, in what is referred to as directionality (Hong and Goda, 2007; Poulos and Miranda, 2022; Shahi and Baker, 2014). In this context, however, only a few validation studies addressed directionality, and those that have done so have focused only on the ratio between the maximum and median intensity (e.g., Burks et al., 2015; Burks and Baker, 2014; Galasso et al., 2020; Teng and Baker, 2019). None have explicitly focused on other directionality characteristics, such as the orientation of maximum horizontal spectral response or its spatial distribution.

The lack of validation studies for the orientation of maximum response in simulated ground motions may partially be attributed to the common belief that the maximum intensity occurs at random, unpredictable orientations for source-to-site distances larger than 5 km. The orientation of maximum response in recorded ground motions has historically been studied by considering the angular distance of this orientation from the strike-normal orientation. In their landmark paper, Somerville et al. (1997) observed that, for sites close to faults and oscillators with periods longer than 0.6 s, the spectral accelerations in the fault-normal orientation tend to be larger than average, which they attributed to radiation patterns of shear waves. Since then, it is well documented that there is a higher probability that the orientation of maximum response is closer to the strike-normal orientation for rupture distances less than 5 km; however, at distances greater than 5 km, most studies

found that the maximum spectral response does not have a preferred orientation (Huang et al., 2008; NEHRP Consultants Joint Venture, 2011; Shahi and Baker, 2014). Recently, Poulos and Miranda (2023a) studied the orientation of maximum spectral response of ground motions in the NGA-West2 database (Ancheta et al., 2014) by measuring and conducting statistical analyses of the angular distance of this orientation from the epicentral transverse orientation (i.e., the orientation of the ground motion transverse component, which is perpendicular to a line connecting each recording station to the epicenter). Using more than 5,000 recorded ground motions, they found that for ground motions recorded in strike-slip earthquakes, there is a tendency for the orientation of maximum response to be close to the epicentral transverse orientation and that, although less pronounced at shorter periods, it gets closer to the transverse orientation as the oscillator period increases. These new findings have also been independently verified in ground motions recorded during recent strike-slip earthquakes not included in the NGA-West2 database (Girmay et al., 2023, 2024; Poulos and Miranda, 2024).

Whilst there have been several studies on directionality of recorded earthquake ground motions, there have been few on directionality of ground motion simulations, and none specifically focusing on the orientation of maximum response. Burks and Baker (2014) suggested a list of parameters that can be used as proxies to validate ground motion simulations. In particular, to evaluate directionality, they recommended computing the ratio of the maximum intensity (RotD100) and the median intensity of all orientations (RotD50) for the simulations and comparing these ratios with those computed from recorded ground motions and empirical models. Using a few records, they found that the variation of median RotD100/RotD50 with changes in oscillator period for broadband simulations, although generally matching the trend of recorded ground motions, tended to result in a more polarized response for long-period oscillators. Similarly, Burks et al. (2015) found that the RotD100 spectra of broadband simulations tended to be notably larger than empirical ground motion prediction models (GMPMs) and that simulations tended to produce more polarized motions compared to empirical predictions at long periods. They also found that broadband simulations tended to produce ground motions with larger amplitudes in the fault-normal orientations and lower amplitudes in the fault-parallel orientations when compared to recorded motions, meaning that simulated ground motions are more polarized than recorded ones. Other recent studies that have evaluated the possible use of simulated ground motions for engineering applications have also found that the simulated motions,

on average, tended to produce larger RotD100/RotD50 ratios at long periods of vibration when compared to recorded motions, and thus tended to polarize response more than recordings (Galasso et al., 2020; Teng and Baker, 2019).

All studies identified above primarily focused on validating the level of polarization of the simulated ground motions by using the RotD100/RotD50 ratio as a proxy and did not study other directionality characteristics. This suggests a gap in existing literature regarding directionality in simulated ground motions and, more specifically, the variation of the level of intensity with changes in orientation or the orientation of maximum response. Therefore, it is of interest to investigate these aspects of directionality in ground motion simulations, particularly in the context of the recent findings by Poulos and Miranda (2023a) for strike-slip earthquakes. At the center of Poulos and Miranda's reasoning for investigating the orientation of maximum response with respect to the epicentral transverse orientation is that S waves from theoretical double couple point sources in a homogenous medium exhibit polarization transverse to the direction of propagation (Aki and Richards, 2009). Thus, evaluating whether this phenomenon is also apparent in physics-based simulations would be important.

This work uses CyberShake Study 15.12 to evaluate directionality in simulated ground motions from strike-slip earthquakes. CyberShake is a physics-based computational study developed by the Southern California Earthquake Center (SCEC) to calculate the seismic hazard for sites in California (Graves et al., 2011; Graves and Pitarka, 2010). This study investigates whether the physics-based simulations sufficiently capture some directionality characteristics observed in recorded earthquake ground motions. More specifically, the orientation of maximum spectral response and the spatial distribution of response for 5%-damped linear elastic oscillators when subjected to these simulated ground motions is studied. The dependence of the orientation of maximum response on rupture variation and oscillator period is investigated. The extent of polarization in the simulated ground motions within the horizontal plane is studied for each period by evaluating spectral accelerations in all non-redundant orientations.

SELECTED GROUND MOTION SIMULATIONS

The simulated ground motions used in this study were obtained from SCEC's CyberShake Study 15.12, which includes ground motion simulations for over 300 stations around the

greater Los Angeles (LA) metropolitan region generated by considering all Uniform California Earthquake Rupture Forecast, Version 2.0 (UCERF2.0) ruptures within 200 km from each station (Graves et al., 2011). For each station, there are over 7,000 ruptures, which in this context refers to a realization of an earthquake of a given magnitude, and 415,000 rupture variations, which refers to a realization of a particular hypocenter and slip distribution within each rupture.

Specifically, this paper uses ground motions simulated at 334 stations from five different rupture variations across two strike-slip ruptures, totaling 1,670 records. The two rupture simulations studied include M_w 6.95 and M_w 7.45 events on the Elsinore fault zone. This major active fault zone is part of the right-lateral strike-slip San Andreas fault system in southern California, stretching over 200 km from the south-east boundary of the LA basin to the border with Mexico (Hull and Nicholson, 1992; Magistrale and Rockwell, 1996). Each of the two rupture simulations studied involve multiple segments of the fault zone, with the smaller magnitude event rupturing the Whittier and Glen Ivy segments (W+GI) and the larger magnitude event rupturing the Glen Ivy, Temecula, Julian, and Coyote Mountain segments (GI+T+J+CM). To investigate the effect of hypocenter location and direction of rupture propagation on the orientation of maximum intensity, different rupture variations (i.e., hypocenter realizations) were chosen such that they initiate at distinctly different hypocenter locations for each rupture. Specifically, for the W + GI rupture, these include hypocenters at the south-most end (i.e., south-to-north rupture propagation), north-most end (i.e., north-to-south rupture propagation), and center (i.e., bilateral rupture propagation). For the GI+T+J+CM rupture, only hypocenters at the south-most and north-most ends were considered. For each rupture variation described above, the velocity seismograms at each station were downloaded and then numerically differentiated to obtain acceleration waveforms, which were then used to compute the relative displacement response of 5%-damped linear elastic single-degree-of-freedom oscillators. See the Data and Resources section of this paper for the specific CyberShake database identifiers of the ground motion simulations used in this study.

ORIENTATION OF MAXIMUM SPECTRAL RESPONSE

CyberShake simulated ground motions provide complete waveforms at a given station in one vertical and two horizontal orientations, much like those in recorded ground motions. In earthquake engineering, the most common measure of ground motion intensity is the

5%-damped response spectral ordinate, which represents the peak response of a single-degree-of-freedom linear-elastic oscillator with a 5% damping ratio. The availability of two orthogonal horizontal components at a station allows the computation of the bidirectional response of an oscillator within the horizontal plane, which represents the trace (or hodograph) of the oscillator's motion when subjected to the ground motion. For example, Figure 1a shows the relative displacement response of a 5%-damped linear-elastic 7 s oscillator subjected to the ground motion generated at station S597 from a simulation of a M_w 6.95 rupture on Elsinore fault (W + GI). Cross-plotting the response in the two orientations shown in Figure 1a results in the hodograph indicated by the red trace in Figure 1b. Having the complete response in two orientations at a given station also allows for the computation of waveforms or spectral ordinates in any desired orientation. For instance, Figure 1c shows the relative displacement waveforms in the transverse and radial orientations.

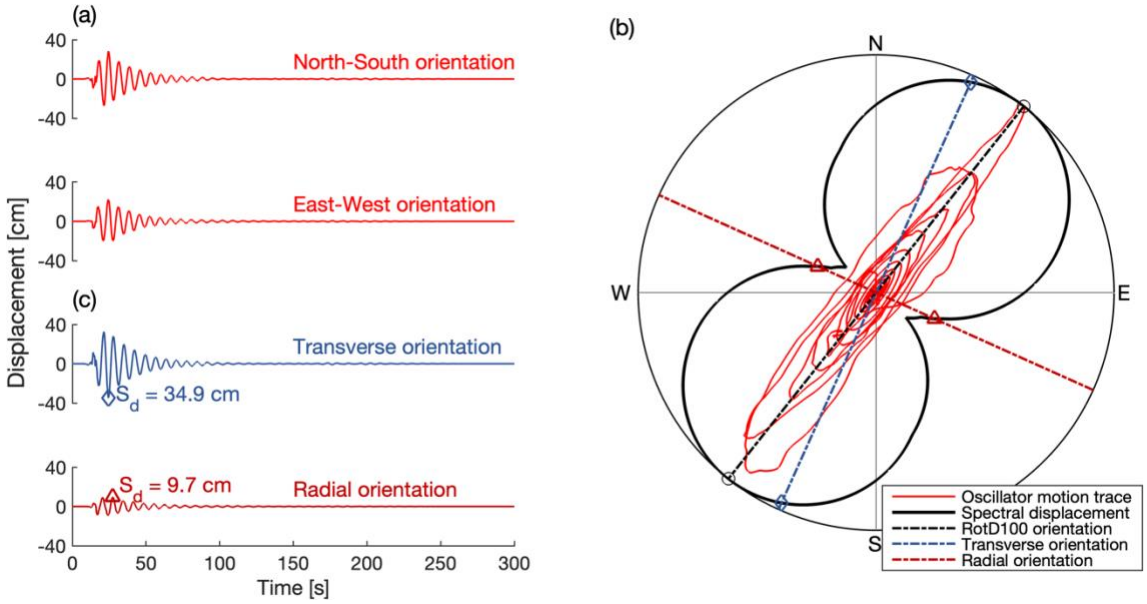

Figure 1. An example of relative displacement response of a 7 s oscillator when subjected to the ground motion generated at station S597 from a simulation of a M_w 6.95 rupture on Elsinore fault (W + GI): (a) relative displacement response of the oscillator in the north-south and east-west orientations; (b) bidirectional response of the oscillator in the horizontal plane (i.e., hodograph) and the corresponding spectral displacement in all orientations, also indicating the peak relative displacement of the oscillator in the transverse and radial orientations; and (c) relative displacement response of the oscillator in the transverse and radial orientations. The circular marker indicates the maximum spectral response, and the diamond and triangular markers indicate the spectral ordinates in the transverse and radial orientations, respectively.

To get a better understanding of directionality in physics-based ground motion simulations, hodographs like that shown in Figure 1 can be computed and studied for all stations. Figure 2a shows the spatial distribution of relative displacement hodographs of 5%-damped linear-

elastic 7 s oscillators subjected to all ground motions generated from a simulation of a M_w 6.95 rupture on Elsinore fault (W + GI). The hodograph in red corresponds to that for station S597 (which was provided as an example in Figure 1), and the green line indicates the rupture trace. The epicenter for the rupture is indicated by the green star. CyberShake Study 15.12 was created to compute hazard curves at multiple sites in southern California, which required generating waveforms at numerous stations with close spacing between them. As a result, the spatial distribution of most stations shown in Figure 2a has a semi-regular grid arrangement, making it particularly valuable to study directionality (in contrast to real-world recording stations, which are often clustered around large urban areas and their corresponding infrastructure). In Figure 2a, the size of each hodograph indicates the station-to-station variation of intensity. It is apparent that the hodographs are largest at stations close to the rupture and epicenter, and their size decreases with increasing rupture distance. The large variation of intensity between stations makes it difficult to identify and compare the shapes of the hodograph. In order to better visualize and compare both the level of polarization and the orientation of maximum response at each station, the relative displacement hodographs can be normalized by the maximum spectral response and scaled to show the bidirectional motion at all stations with the same peak amplitude. For example, Figure 2b shows the normalized version of Figure 2a, which permits a clearer comparison of hodograph shapes for the event.

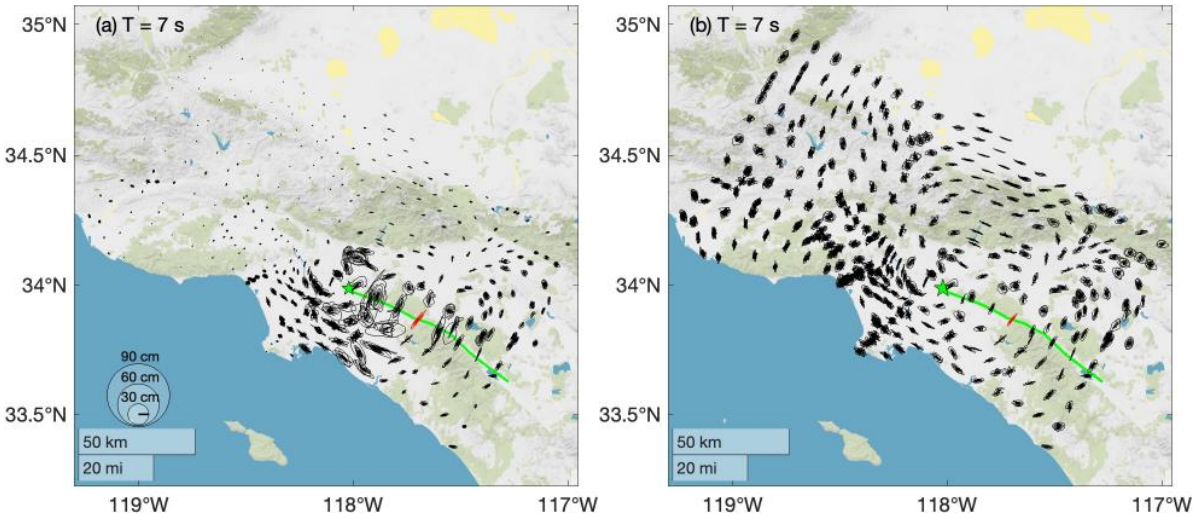

Figure 2. Spatial distribution of relative displacement hodographs of 5%-damped linear elastic oscillators with periods T = 7 s subjected to simulated ground motions generated from a M_w 6.95 rupture on Elsinore fault (W + GI). The hodograph sizes are (a) relative, such that the size of each hodograph indicates the station-to-station variation in the ground motion intensity, and (b) normalized and scaled to show all stations with the same peak amplitude. The hodograph in red is for station S597 (see Figure 1b).

Figure 3 shows the normalized relative displacement hodographs of 5%-damped linear-elastic oscillators subjected to ground motions generated from the same rupture as that shown in Figure 2, but for four different oscillator periods (3, 5, 7, and 10 s). In Figure 3, stations near each other tend to have similar bidirectional responses, generally characterized by being circumscribed by an approximate elliptical shape, regardless of the oscillator period considered. As the oscillator period increases, its response becomes "cleaner" and more elliptical (i.e., with notably larger major axes relative to minor axes) at all distances from the rupture. This implies that there is an increase in the level of polarization in the oscillator's bidirectional response as its period of vibration increases. Additionally, adjacent stations tend to have similar orientations of the principal axes of the ellipse, suggesting that the orientation of maximum response is not entirely random and that the motions have some preferred orientation of maximum response. The bidirectional responses in Figure 3 are consistent with those observed in oscillators subjected to recorded earthquake ground motions from strike-slip earthquakes, as noted by Poulos and Miranda (2023a) and others (Girmay et al., 2023, 2024).

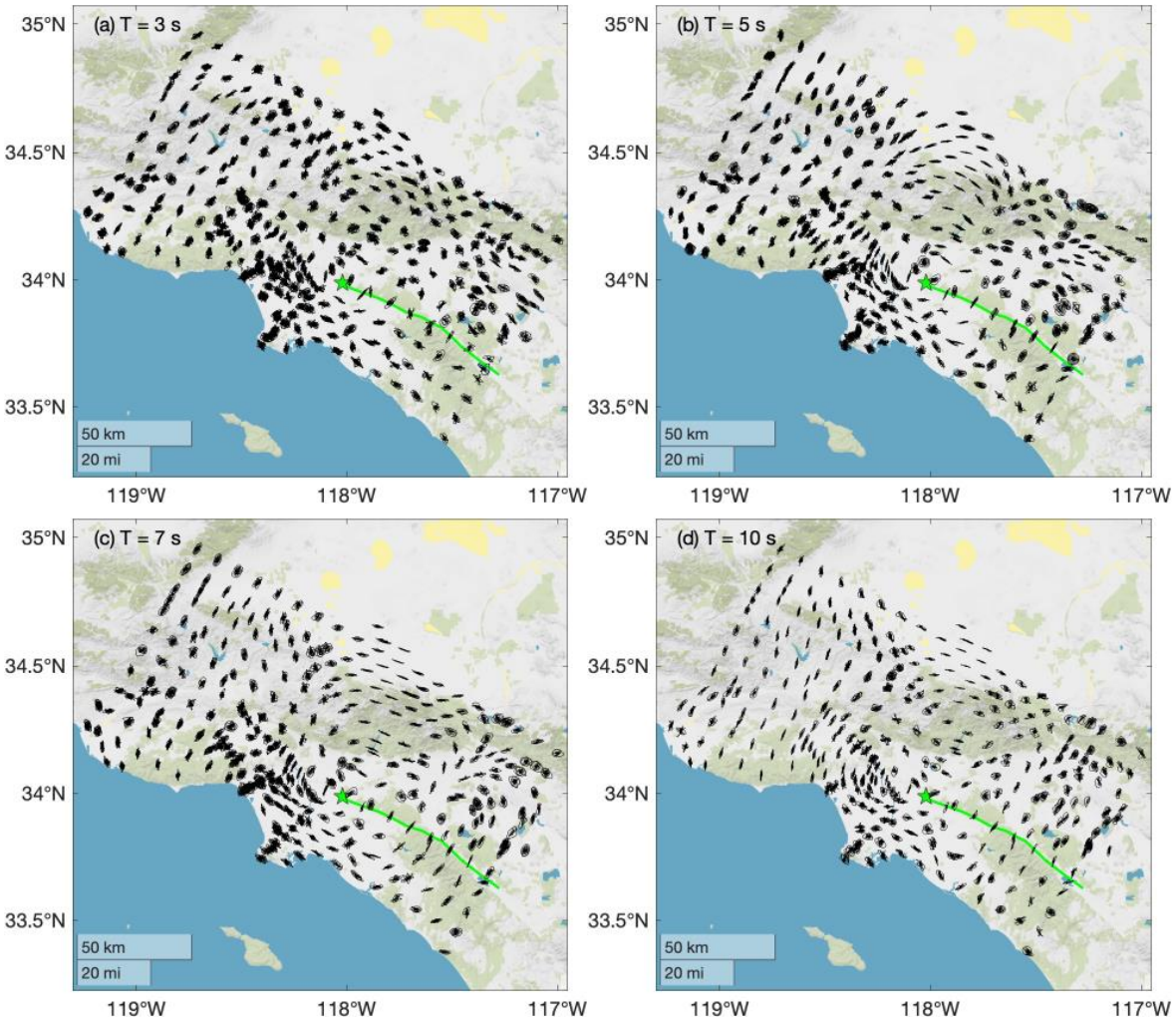

Figure 3. Normalized relative-displacement hodographs of 5%-damped linear elastic oscillators subjected to ground motions generated from a simulation of a M_w 6.95 rupture on Elsinore fault (W + GI) for oscillators having periods of (a) T = 3 s, (b) T = 5 (s), (c) T = 7 s, and (d) T = 10 s. The epicenter is indicated by the green star, and the rupture propagates from north to south along the fault trace shown by the green line.

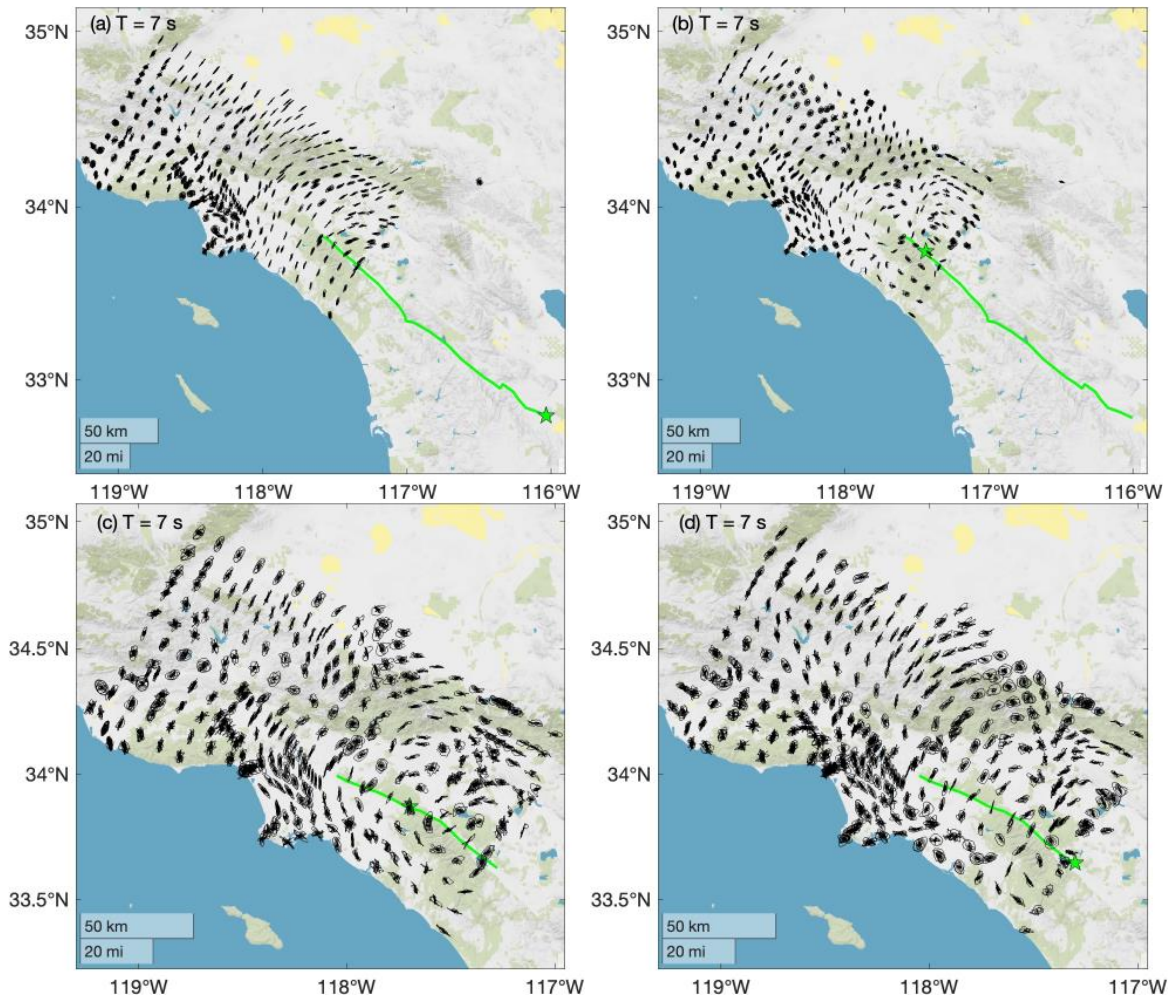

Figure 4. Normalized relative-displacement hodographs of 5%-damped linear elastic oscillators with periods T = 7 s subjected to ground motions generated from simulation of ruptures on Elsinore fault with (a) M_w = 7.45 and rupture running south-north, (b) M_w = 7.45 and rupture running north-south, (c) M_w = 6.95 and bilateral rupture, and (d) M_w = 6.95 and rupture running south-north. Ruptures in (a) and (b) consist of GI + J + T + CM segments, while ruptures in (c) and (d) consist of W + GI segments. The green line indicates the rupture trace, and the epicenter is indicated by the green star.

Should these observations result from a physical phenomenon, it would be expected that similar observations would hold for both recorded and simulated ground motions, and additionally for other realizations of simulated ruptures with the same faulting mechanism. Figure 4 shows the bidirectional response of 7 s oscillators subjected to simulated ground motions generated due to four different rupture scenarios on the Elsinore fault. The surface projection of the rupture trace for each scenario is again indicated by the green line, and the green star indicates the epicenter. The bidirectional oscillator responses to ground motions from each rupture simulation show trends similar to those observed in Figure 3. Most stations tend to have an elliptical response, and the response of adjacent stations remains similar regardless of the earthquake's magnitude, rupture length, or location of the

epicenter. The stability of this observation across different strike-slip rupture realizations is consistent with that observed for ground motions recorded during strike-slip earthquakes. For example, Poulos and Miranda (2023a) observed similar bidirectional responses for strike-slip earthquakes in the NGA-West2 database, such as the 1991 M_w 7.1 Hector Mine earthquake. More recently, Girmay et al. (2023, 2024) noted similar observations for the 2022 M_w 6.4 Ferndale earthquake and the 2023 Türkiye earthquake doublet, respectively.

For a record that has waveforms available in two orthogonal horizontal orientations, the two waveforms can be combined to compute the peak oscillator response at any specific azimuth and rotated incrementally to obtain the variation of spectral ordinates in each nonredundant orientation (i.e., a range of azimuths of 180°, see Figure 1b) (Boore, 2010). Within the nonredundant orientations, the 100th percentile of spectral response is referred to as RotD100 (also known as the maximum spectral response), and the 50th percentile is referred to as RotD50 (also known as the median spectral response) (Boore, 2010). Thus, the orientation of maximum spectral response corresponds to the azimuth at which the RotD100 intensity occurs while the RotD50 orientation can occur at two or more different orientations. Visually, the maximum spectral response at each station shown in Figures 2 – 4 corresponds to the point in each hodograph that is furthest away from the resting position of the oscillator (as illustrated in Figure 1b).

As discussed in the introduction, most, if not all, prior studies that have studied the directionality of simulated ground motions have focused on whether the ratio between the maximum response and the median response with the horizontal plane is consistent with that computed from recorded ground motions. The median of this ratio has a stable and known variation with changes in the period of vibration of the oscillator (Burks and Baker, 2014), and thus is often used as a proxy in ground motion simulations validation exercises to evaluate directionality (Burks et al., 2015; Burks and Baker, 2014; Galasso et al., 2020; Teng and Baker, 2019). More recent findings by Poulos and Miranda (2023a) have identified that for strike-slip earthquakes, the orientation of maximum spectral response tends to be close to the transverse orientation. They found that this observation is less pronounced at short periods but becomes apparent with increasing period. Therefore, it would be important to verify whether the simulated ground motions exhibit orientations of maximum response that are consistent with those observed in recorded ground motions.

In their study of the orientation of maximum spectral response in recorded ground motions, Poulos and Miranda (2023a) defined the angle between the orientation of RotD100 and the epicentral transverse orientation (i.e., the orientation orthogonal to a line connecting the epicenter to the station) as $\alpha \in [-90°, 90°]$. Measured relative to the transverse orientation, this angle is negative if RotD100 orientation is clockwise or positive if counterclockwise. A similar measure of angular difference between the transverse and RotD100 is $|\alpha| \in [0°, 90°]$, which does not distinguish between the clockwise or counterclockwise orientation of RotD100 with respect to the transverse orientation. In this study, distinguishing between clockwise or counterclockwise is not considered since, according to Poulos and Miranda (2023a), the mean variation of intensity is symmetric with respect to the orientation of RotD100. Therefore, the angular difference $|\alpha|$ is used.

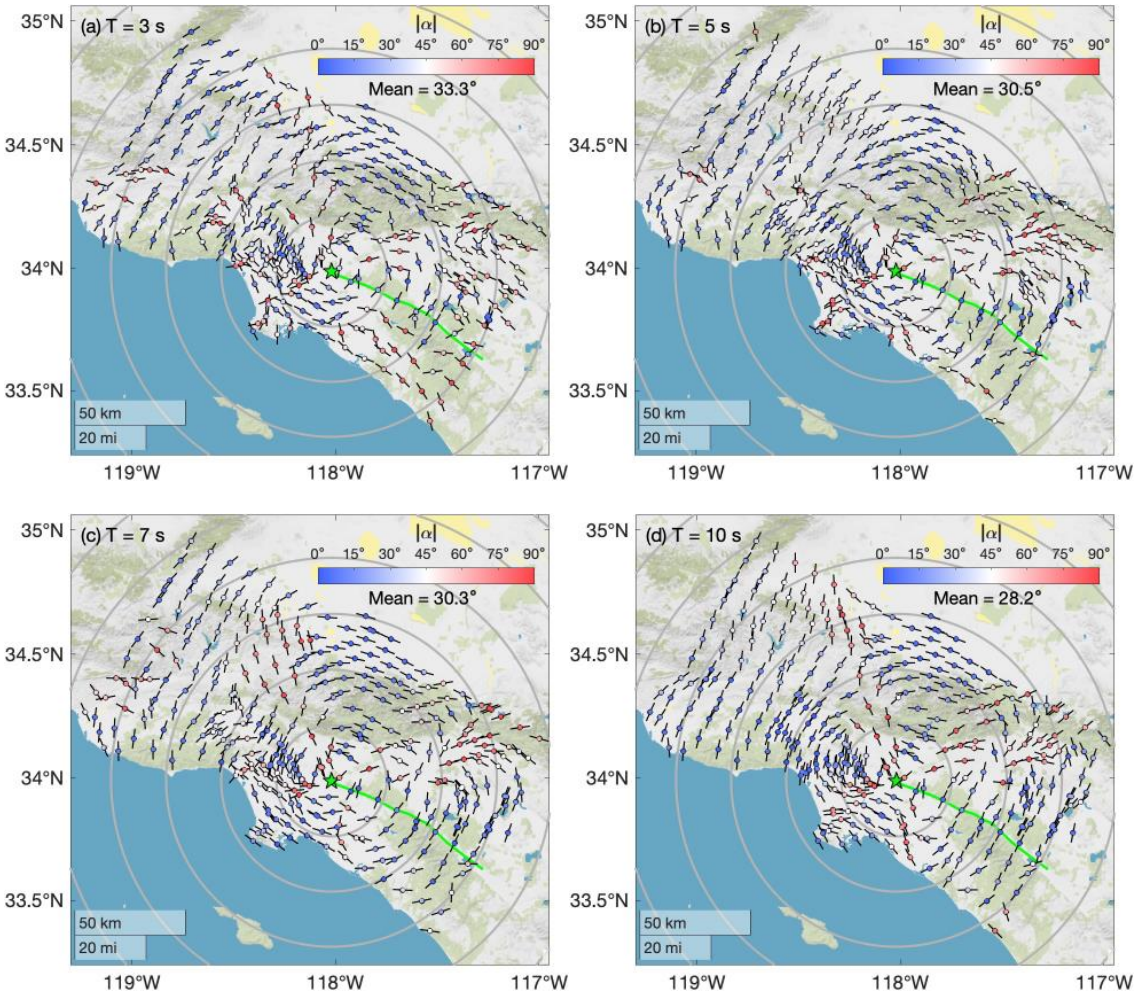

Figure 5. Orientation of maximum spectral response of 5%-damped linear elastic oscillators with periods of (a) 3 s, (b) 5 s, (c) 7 s, and (d) 10 s, as indicated by the short black line segments at each station (indicated by a circle), and their angular difference from the transverse orientation, as indicated by the color inside each circle. Each station is subjected to ground motions generated from a simulation of a M_w 6.95 rupture on the Elsinore fault (W + GI). The large concentric grey circles centered around the epicenter indicate epicentral transverse orientations.

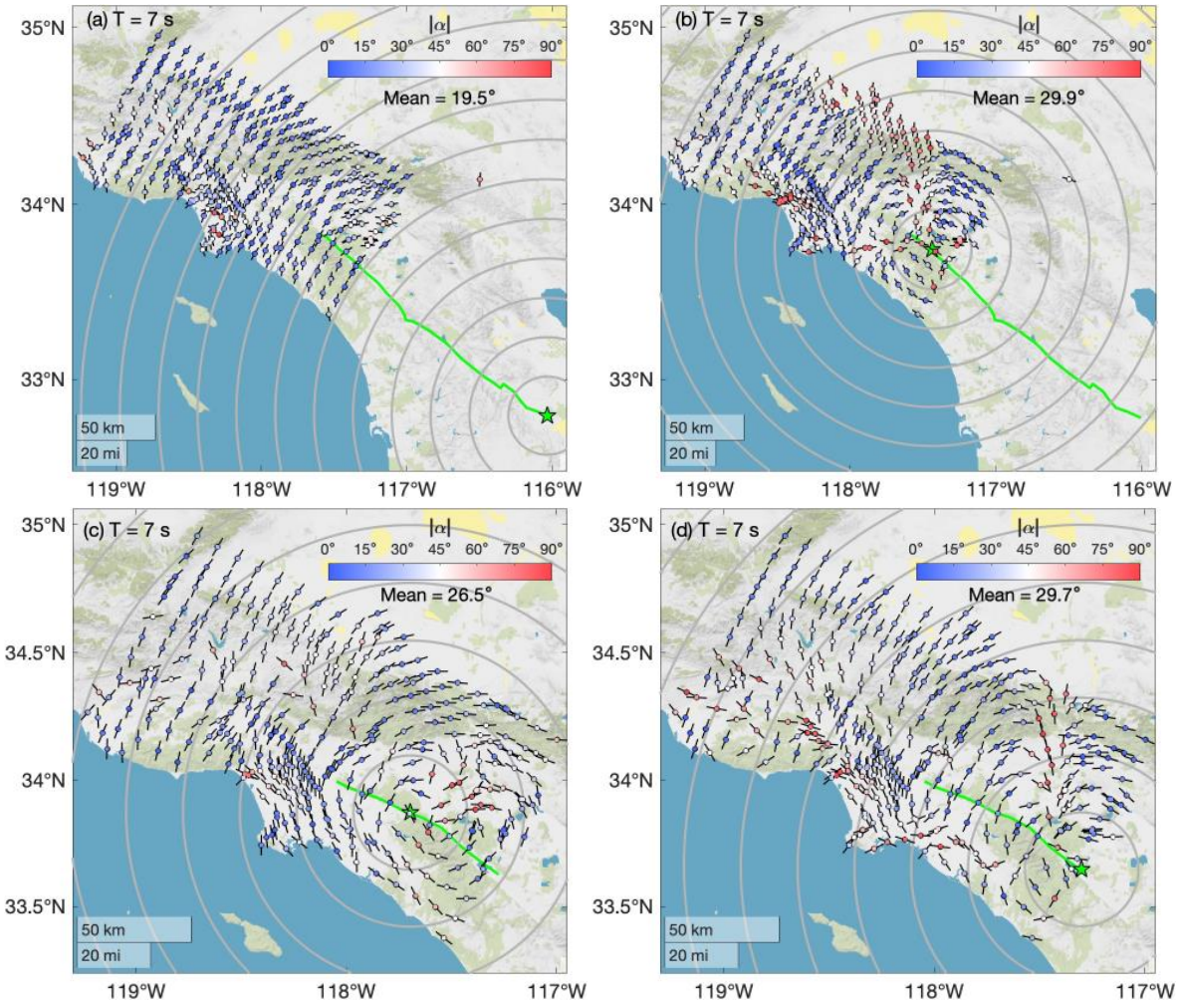

Figure 6. Effect of rupture variation on the orientation of maximum spectral response of 5%-damped linear elastic oscillators with periods of 7 s. The orientation of maximum spectral response at each station is indicated by the short black line segments at each station, and the angular difference from the transverse orientation is indicated by the color inside each circle. The large concentric grey circles centered around the epicenter indicate the epicentral transverse orientations.

Figure 5 uses short black line segments to indicate the RotD100 orientation at each station for oscillators with four different fundamental periods subjected to ground motions generated from a simulated M_w 6.5 earthquake on the Elsinore fault (W + GI). The color inside the circles at each station indicates the angular difference between the RotD100 orientation and the epicentral transverse orientation, with red tones signifying RotD100 orientations closer to the radial orientation and blue tones signifying RotD100 orientations closer to the transverse orientation. Generally, the orientations of the short black line segments in Figure 5 are typically similar for adjacent stations and, for most stations, tend to form a circular pattern around the epicenter. As the period of vibration of the oscillators increases, the circular pattern around the epicenter becomes more apparent. Most stations

311 also have circles with blue tones, suggesting that, for most stations, the RotD100
312 orientation occurs close to the transverse orientation across all four periods shown in the
313 figure. Furthermore, as the oscillator period increases, more stations become blue colored,
314 indicating that more stations have RotD100 orientations that occurred close to the
315 transverse orientation. To better understand the effects of rupture variations, Figure 6 shows
316 the spatial distribution of $|\alpha|$ but for four different rupture realizations on the Elsinore fault
317 for a single oscillator period of 7 s. Much like what is observed in Figure 5, most stations
318 in Figure 6 also have blue-toned circles, suggesting that the RotD100 orientation remains
319 close to the transverse orientation regardless of rupture length, rupture initiation, or rupture
320 direction. These observations are consistent with those made from recorded earthquake
321 ground motions.

322 Prior studies on ground motions recorded from recent strike-slip earthquakes (Girmay et
323 al., 2023, 2024; Poulos and Miranda, 2023a) have found that the empirical probability
324 distribution of $|\alpha|$ deviates significantly from a uniform distribution and has a predictable
325 pattern, with larger density occurring at lower $|\alpha|$ values. Therefore, should the simulated
326 ground motions appropriately capture directionality characteristics, then the empirical
327 distribution of $|\alpha|$ for the simulated ground motions should follow the same, or at least a
328 very similar, pattern as that from recorded ground motions. While Figures 5 and 6 use
329 colors to indicate the spatial distribution of $|\alpha|$ in the simulated ground motions, Figure 7
330 presents the empirical probability distribution of $|\alpha|$ for four oscillators subjected to ground
331 motions generated from different earthquake ruptures simulated on the Elsinore Fault. The
332 top row shows probability distributions of $|\alpha|$ for four different periods of vibration
333 computed from a single realization that ruptures the Elsinore fault from north to south
334 involving the Whittier and Glen Ivy segments; similarly, the second row aggregates the
335 probability distribution of $|\alpha|$ considering all five rupture variations considered in this
336 study for a total 1,670 simulated ground motions. Inset in each panel of the figure is the
337 mean $|\alpha|$ and total number of records used for each case.

338 Figure 7 shows that the empirical distribution of $|\alpha|$ is skewed towards small values of $|\alpha|$
339 for all oscillator periods, with the greatest density between 0° and 30°. As the oscillator
340 period increases, the distribution gets more skewed, as indicated by the increased density
341 at lower $|\alpha|$ and by the increase in the skewness coefficient. This observation is true for
342 both the single M_w 6.95 rupture on the W+GI segments and for the aggregated data using

simulated ground motions from all ruptures. If RotD100 was equally likely to occur in any orientation with respect to the transverse orientation, then the observed distribution would have been uniform as indicated by the dashed blue horizontal line, and the mean $|\alpha|$ would be 45°. However, the distributions are highly skewed and the mean $|\alpha|$ for each period is notably below 45°, indicating that the orientation of RotD100 tends to occur close to the epicentral transverse orientation. These empirical probability distributions are consistent with the findings for ground motions recorded during strike-slip earthquakes, suggesting that the physics-based simulations generally capture the main features of the directionality effects present in recorded ground motions.

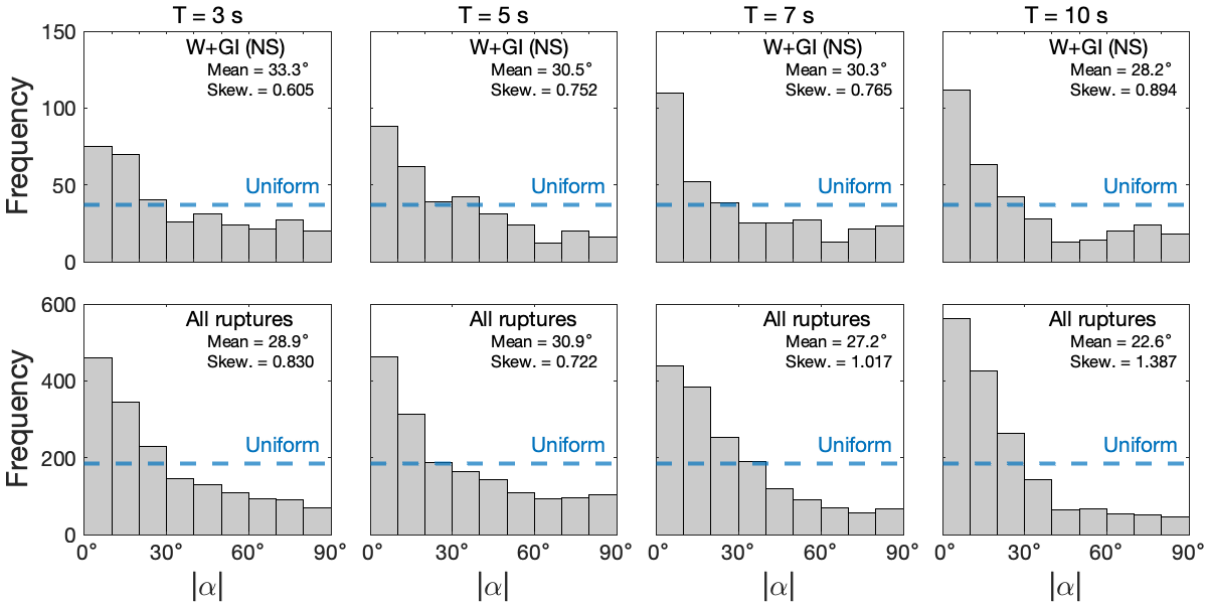

Figure 7. Histograms of the angular difference between the transverse orientation and the RotD100 orientation for oscillators subjected to simulated ground motions from different rupture variations simulated on the Elsinore Fault. The top row presents results for a simulated M_w 6.95 event on the W + GI segments rupturing north-to-south (NS), whilst the bottom row presents results computed from simulations of five different realizations, comprised of three M_w 6.95 ruptures on the W + GI segments and two M_w 7.45 ruptures on the GI + J + T + CM segments. The dotted line represents the histogram should the orientation of RotD100 be equally likely to occur at any orientation with respect to the transverse orientation. Each panel indicates the mean $|\alpha|$ and the skewness coefficient. A total of 334 records were used for the top row, and 1,670 were used for the bottom row.

As previously mentioned, one trend that has been found in ground motions recorded during strike-slip earthquakes is the tendency for the mean values of $|\alpha|$ to decrease with increasing oscillator period. In other words, in recorded strike-slip earthquakes, it has been found that the orientation of RotD100 tends to get closer to the transverse orientation as the period of vibration of the oscillator increases. This is often attributed to wave scattering

since higher frequencies have shorter wavelengths, which makes them more susceptible to heterogeneities in the Earth's crust. To check whether this trend is observed and is similar in the physics-based ground motion simulations, Figure 8 plots the variation of mean $|\alpha|$ as a function of oscillator period for five different rupture variations on the Elsinore fault. Figure 8a presents the results for variations that ruptured the W + GI segments, whilst 8b shows the results for variations that ruptured the GI+T+J+CM segments. Also included in the figure and indicated by the black line is the mean $|\alpha|$ for 1,962 ground motions recorded during strike-slip earthquakes from the NGA-West2 database as computed by Poulos and Miranda (2023a). There are three main observations to note from this figure. First, the variation of mean $|\alpha|$ on different variations of the smaller rupture (W + GI) is more similar to each other than it is in the larger rupture (GI+T+J+CM). Second, mean $|\alpha|$ follows similar trends for different rupture realizations, where the RotD100 orientation generally gets closer to the transverse orientation as the period of vibration of the oscillator increases, suggesting that the descending trend is a stable characteristic regardless of the direction of rupture propagation. Third, the mean $|\alpha|$ is consistently below 45° for all rupture variations, suggesting that the orientation of RotD100 tends to occur relatively close to the transverse orientation, which is consistent with the behavior observed in recorded ground motions in the NGA-West2 database. This is further highlighted in Figure 9, which indicates that the probability that $|\alpha|$ falls between 0° and 30° is more than double than that of falling between 30° and 60° or between 60° and 90° for most oscillator periods. The findings in Figures 8 and 9 generally follow the trends observed for real recorded ground motions by Poulos and Miranda (2023a) and Girmay et al. (2023), suggesting that the physics-based simulations exhibit directionality effects that, in general, are consistent with those observed in recorded ground motions.

It is important to note that the significant decrease in the probability that the RotD100 intensity occurs between 0° and 30° from the transverse orientation for periods of vibration between 0 – 1 s, followed by a rapid increase after 1 s, is more accentuated in the simulated ground motions when compared to that observed in recorded ground motions. This may be attributed to the hybrid broadband method used to generate the waveforms, which combines deterministic and semi-stochastic approaches. More specifically, the method for simulation (Graves et al., 2011; Graves and Pitarka, 2010) is deterministic for frequencies below 1 Hz and incorporates a theoretically robust representation of fault rupture and wave

propagation. For frequencies above 1 Hz, the method uses a stochastic representation of source radiation combined with a simplified theoretical representation of wave propagation and scattering effects (Graves and Pitarka, 2010), which seems to adequately capture the probabilities in Figure 9 given the similarity to the probabilities reported by Girmay et al. (2023). Above 2 s, the probabilities are consistent with real ground motions, where the physics dominates (i.e., the polarization of S-waves that result in the orientation of RotD100 being close to the transverse orientation is apparent, and wave scattering effects are not as significant). However, the rapid increase in the probability that RotD100 in simulated ground motions falls between 0° and 30° from the transverse orientation between 1 s and 2 s may be artificially large due to the transition between the stochastic and deterministic approaches.

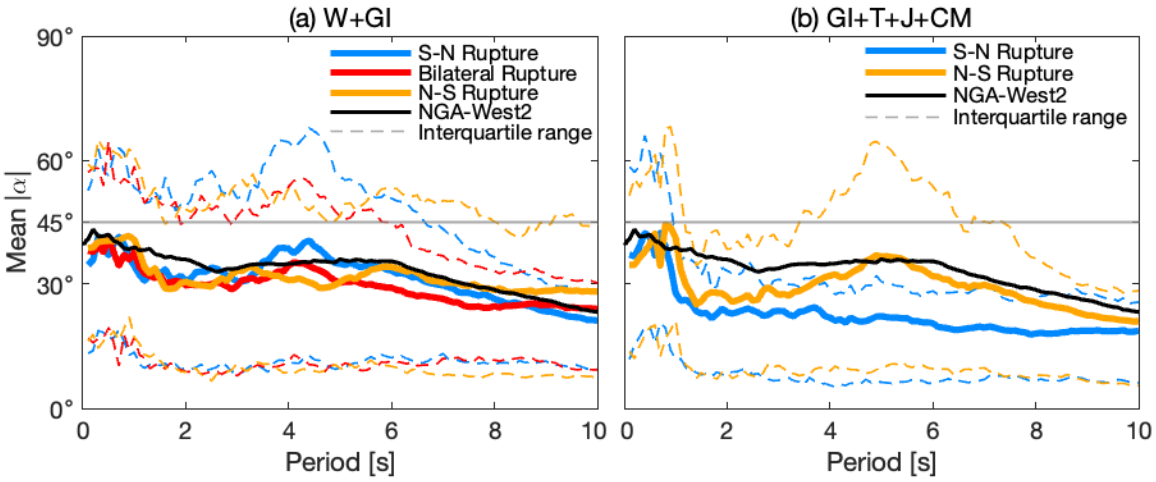

Figure 8. Effect of the period of vibration of the oscillator on the mean angular difference between the orientation of RotD100 and the transverse orientations for five different rupture variations on the Elsinore fault's (a) W + GI segments, and (b) GI + T + J + CM segments. The solid lines present the mean angular difference whilst the dashed lines present the interquartile range. Results for variations that ruptured south-to-north (S-N) are shown in blue, while yellow is used for variations that ruptured north-to-south (N-S). The black line shows the mean angular difference for strike-slip records in the NGA-West2 database, as computed by Poulos and Miranda (2023a).

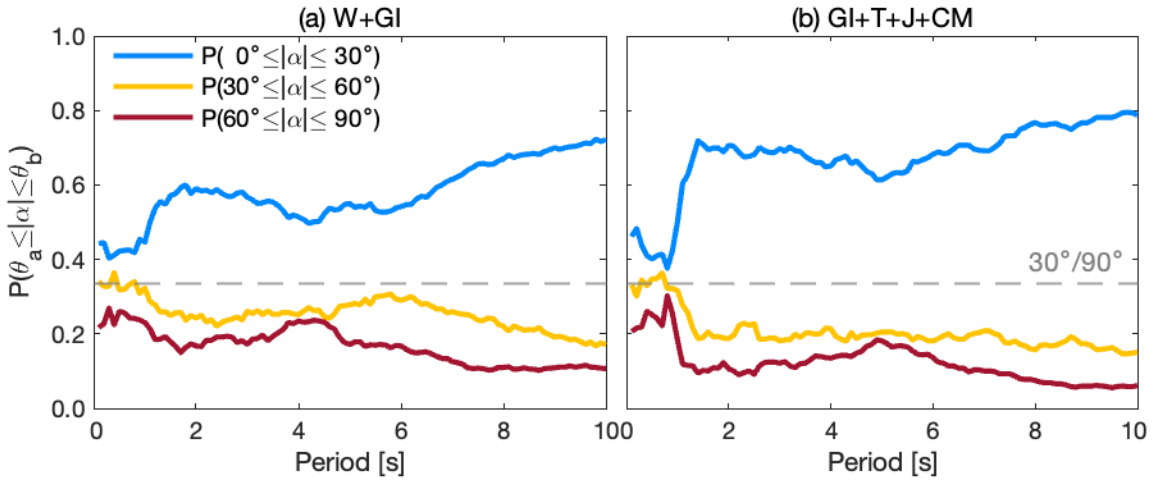

Figure 9. Probability of the angular difference between the orientation of RotD100 and the transverse orientation occurring between [0°, 30°], [30°, 60°], and [60°, 90°] for all rupture variations considered in this study on Elsinore fault segments (a) W + GI, and (b) GI + T + J + CM.

While studying ground motion directionality of spectral ordinates in the 2023 Türkiye earthquake, Girmay et al. (2023) found that the mean $|\alpha|$ at a given period remains relatively constant for Joyner-Boore distances up to the maximum studied (around 400 km). Similar findings were observed for the 2022 Ferndale earthquake, where the epicentral distance was found to have a minimal effect on the distribution of $|\alpha|$ with the exception of the near field region (Girmay et al., 2024). This suggests that an approximately constant mean $|\alpha|$ across a wide range of distances is a stable characteristic of ground motion directionality in recorded motions, so it is important to verify whether simulated ground motions also exhibit this trend.

Figure 10 shows the possible effect of rupture distance on $|\alpha|$ for oscillators with periods of 3 s and 10 s, located at stations where rupture distance information is available. The locally weighted scatter plot smoothing (LOWESS) curve, which is indicated by the blue line, represents the change in mean $|\alpha|$ with increasing rupture distance. On the right-hand side of the figure is the corresponding empirical distribution of $|\alpha|$ and its mean. This figure shows that the LOWESS curve for each oscillator period remains relatively constant across all rupture distances, suggesting that the rupture distance does not substantially influence the orientation of RotD100 with respect to the transverse orientation. Additionally, the scatter points tend to be more concentrated towards the bottom third of the figure, which is further indicated by the histograms on the right that get more skewed with increasing period, signifying that the orientation of RotD100 gets closer to the transverse orientation with increasing period. These observations and trends are consistent with those observed

in recorded ground motion, suggesting that the physics-based simulations exhibit realistic directionality characteristics.

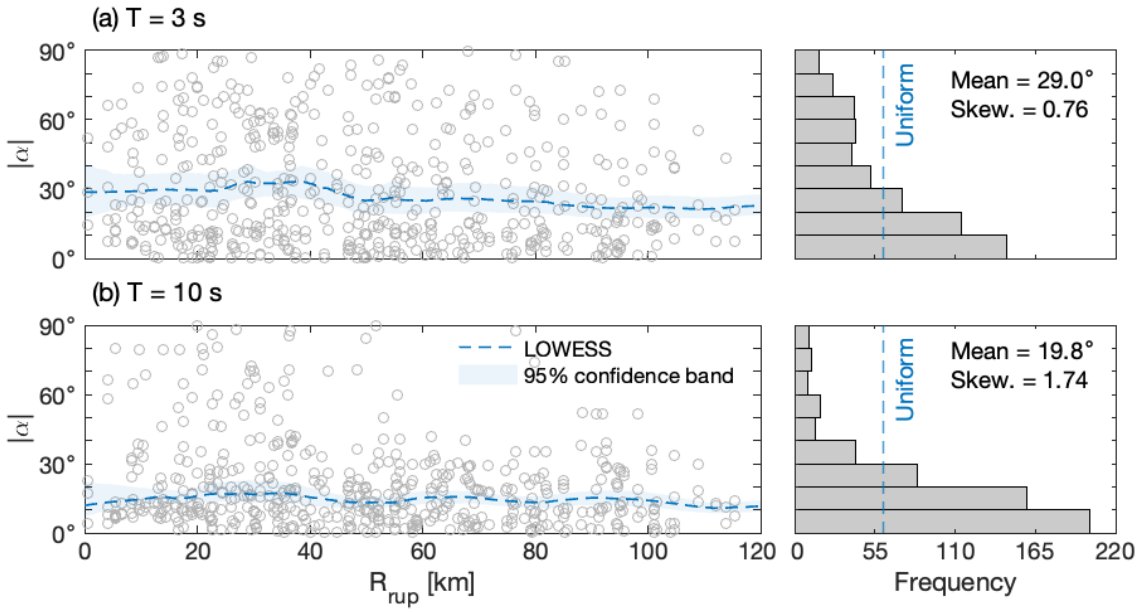

Figure 10. Evaluation of the possible influence of rupture distance on the angular difference between the orientation of RotD100 and the transverse orientation for (a) T = 3 s, and (b) T = 10 s. The dashed lines represent the locally weighted scatterplot smoothing (LOWESS), and the shaded band represents the 95% confidence band. The results presented consider all stations across all rupture variations considered in this study that had rupture distances available in the CyberShake study database (a total of 550 records). For each oscillator period, histograms of the angular difference between the transverse and RotD100 orientations are presented on the right.

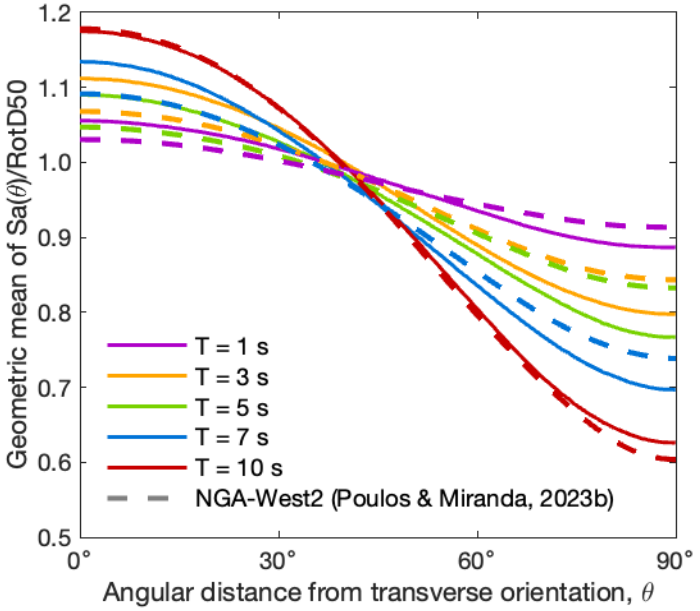

Figure 11. Effect of the angular distance from the transverse orientation on the geometric mean ratio of the spectral response at a given angle from the transverse orientation and the RotD50 intensity for all rupture variations considered in this study. The solid lines represent geometric means of the simulated ground motions for different oscillator periods, whilst the dashed lines represent the results for ground motions recorded during strike-slip earthquakes in the NGA-West2 database (Poulos and Miranda, 2023b).

ORIENTATION-SPECIFIC SPECTRAL ACCELERATIONS

In the previous section, it has been shown that the orientation of RotD100 for physics-based simulations tends to occur close to the epicentral transverse orientation, which is consistent with observations from recorded ground motions. However, another aspect of directionality that has not been previously studied for physics-based simulated ground motions is the variation of ground motion intensity with changes in orientation within the horizontal plane. So, it is important to study this and compare the findings to those from recorded ground motions.

Poulos and Miranda (2023b) found that orientation-specific horizontal spectral accelerations for ground motions recorded from strike-slip earthquakes have generally stable characteristics when computed as a function of the angular distance from the transverse orientation and normalized by the associated orientation-independent median intensity (RotD50). Here, their approach is used to investigate whether the orientation-specific spectral accelerations for simulated ground motions exhibit a similar variation to that observed in recorded ground motions when computed as a function of the angular distance from the transverse orientation.

Figure 11 shows the effect of angular distance from the transverse orientation on the geometric mean ratio of spectral response at a given angle θ from the transverse and the RotD50 intensity (i.e., $Sa(\theta)/RotD50$). The solid lines indicate the geometric mean of $Sa(\theta)/RotD50$ for different oscillator periods subjected to simulated ground motions for all rupture variations considered in this study. Also included in the figure and indicated by the dashed lines are the corresponding geometric mean of $Sa(\theta)/RotD50$ for 1,962 ground motions recorded during strike-slip earthquakes from the NGA-West2 database (Poulos and Miranda, 2023b). Figure 11 shows that the general shape of $Sa(\theta)/RotD50$ for the simulated ground motions follows the general trend of recorded ground motions. At long periods, and more specifically at 10 s, the geometric mean of $Sa(\theta)/RotD50$ for the simulated ground motions agrees closely with that of the NGA-West2 records, especially at angles within 60° from the transverse orientation. With decreasing periods, the geometric mean of $Sa(\theta)/RotD50$ somewhat deviates from that for the recorded ground motions, although the general shape is maintained. The difference between the simulated and recorded ground motions in the short period range may be attributed to wave scattering. Specifically, there is more wave scattering at higher frequencies (i.e., short periods), which

may not be well captured in the physics-based simulations, which use a semi-stochastic method coupled with simplified scattering effects in the high frequencies. However, in the lower frequencies (i.e., as the oscillator period increases), wave scattering effects become less important, and physics-based simulations exhibit directionality characteristics consistent with those of recorded ground motions.

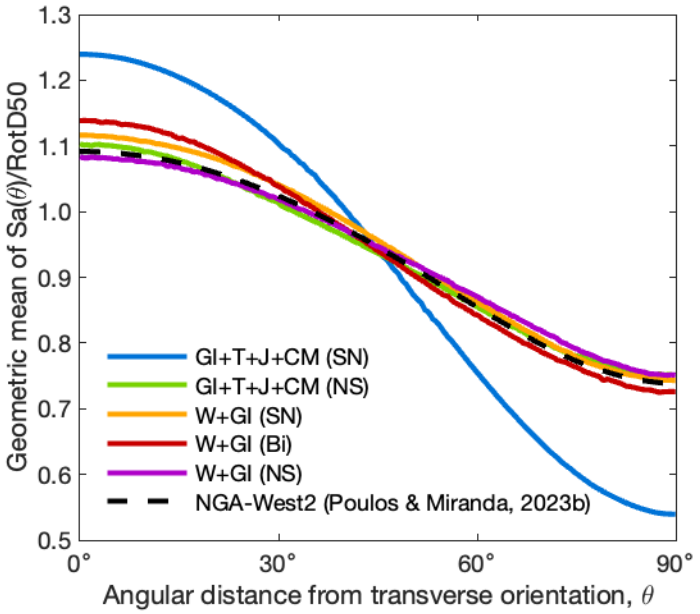

Figure 12. Geometric mean ratio of the spectral response at a given angle from the transverse orientation and the RotD50 intensity for 7 s oscillators as a function of the angular distance from the transverse orientation. The solid lines represent different rupture variations, while the dashed line shows the results for ground motions recorded during strike-slip earthquakes in the NGA-West2 database (Poulos and Miranda, 2023b).

A measure of the level of polarization at different periods can be determined from Figure 11 by comparing the ratio of $Sa(\theta)/RotD50$ at $\theta = 0°$ and $\theta = 90°$. This ratio approximates how much larger the intensity in the major response axis is compared to that in the minor response axis. Therefore, the larger this ratio, the greater the level of polarization in the oscillator response. Figure 11 shows that, except for oscillators with periods of 10 s, the simulated ground motions have a geometric mean of $Sa(0°)/RotD50$ greater than those of records in the NGA-West2 database, whilst also having $Sa(90°)/RotD50$ less than those of records in the NGA-West2. This indicates that the simulated ground motions have a level of polarization that is, on average, greater than that observed in recorded ground motions.

Figure 12 shows the geometric mean of $Sa(\theta)/RotD50$ of 7 s oscillators as a function of angular distance from the transverse orientation for each simulated rupture variation. Also

shown is the geometric mean for ground motions recorded during strike-slip earthquakes in the NGA-West2 database. From this figure, it is apparent that, in general, the $Sa(\theta)/RotD50$ ratio is relatively consistent regardless of rupture variation and generally agrees well with real ground motions in the NGA-West2 database. However, one notable exception is the GI+T+J+CM (SN) rupture realization, which exhibits a much larger level of polarization compared to the NGA-West2. The higher level of polarization in this case can be explained by the location of most stations relative to the location of the epicenter in that particular rupture. More specifically, the epicenter for the GI+T+J+CM (SN) rupture (see Figure 6a) occurs such that the azimuth of each station relative to the epicenter is similar for all stations, which results in the transverse orientation at each station generally coinciding. Ultimately, this results in most stations having very similar levels of response polarization, which also produces a higher mean polarization. Nonetheless, the results in Figures 11 and 12 show that the physics-based simulations, despite resulting in a somewhat larger level of polarization than expected, still have variations in intensity with changes in orientation that are consistent with those of recorded ground motions.

SUMMARY AND CONCLUSIONS

This study used simulated ground motions obtained from CyberShake Study 15.12 to investigate several aspects of the directionality in simulated ground motions. The observations for simulated ground motions were compared to those from ground motions recorded during strike-slip earthquakes. Linear elastic oscillators at more than 300 locations were subjected to simulated ground motions from five rupture realizations. Then, the following aspects were carefully studied: (1) variation of the level of directionality with changes in the period of the oscillators; (2) possible effect of distance to the source on the level of polarization; (3) orientation of maximum oscillator (i.e., spectral) response and its spatial distribution; and (4) variation of the level of ground motion intensity as one rotates away from the transverse orientation. Additionally, the possible effects of rupture variation (i.e., rupture length, point of initiation of the rupture, and direction of rupture propagation) on directionality were investigated and compared to trends observed in recorded ground motions.

The orientation of maximum response of 5%-damped single-degree-of-freedom oscillators subjected to ground motions from physics-based simulated strike-slip ruptures tends to occur systematically close to the epicentral transverse orientation, consistent with recent

findings for records obtained from strike-slip earthquakes. Oscillator hodographs at stations close to each other were found to be similar over the spatial region that was studied. The hodographs at neighboring stations tended to become even more similar and polarized with increasing period. In addition to the increase in polarization, the orientation of maximum intensity got closer to the epicentral transverse orientation as the oscillator period increased. The orientation of maximum spectral response remained close to the transverse orientation for all rupture variations considered. This is consistent with previous observations for ground motions recorded during strike-slip earthquakes with magnitudes larger than or equal to five.

Lastly, orientation-specific spectral accelerations normalized by the median intensity from all orientations of the simulated ground motions, when computed as a function of angular distance from the transverse orientation, were generally found to exhibit variations consistent with records in the NGA-West2 database. At long periods, where the wave scattering effects are less important, the physics-based simulations exhibit mean variation of intensity as a function of the angular distance from the transverse orientation that closely aligns with that from recorded ground motions. However, at short periods, where the physics-based simulations use semi-stochastic methods and simplified scattering effects, the simulated waveforms exhibit a level of polarization that is greater than that observed in recorded ground motions, suggesting that ground motions simulated with the hybrid approach are not fully able to reproduce all the wave scattering that occurs near the surface. This might be because the crustal structure used in the CyberShake Study 15.12 did not consider shear wave velocities lower than 500 m/s.

Ground motion simulations have the potential to play an important role in earthquake engineering and design, especially in the absence of suitable real records (such as for short source-to-site distances and large magnitudes). While numerous prior validation studies focused on various features of these simulated ground motions, none solely focused on directionality. The findings in this paper demonstrate that the physics-based ground motions for strike-slip earthquakes, despite their higher-than-expected level of polarization at short periods, sufficiently capture stable directionality characteristics observed in recorded ground motions. These results provide more confidence in using simulated ground motions for appropriate engineering applications, particularly for structures with periods longer than 1 s where directionality effects are more important.

DATA AND RESOURCES

All simulated ground motions used in this study were obtained from CyberShake Study 15.12 (https://strike.scec.org/scecpedia/CyberShake_Study_15.12). Unique database identifiers for each rupture realization used are summarized below. Map figures in this paper used tiles by MapTiler and base-map data by OpenStreetMap.

Fault	Source_ID	Rupture_ID	Rup_Var_ID	ERF_ID	Rup_Var_Scenario_ID	SGT_Variation_ID
Elsinore (W+GI) S-N Rupture	17	0	0	36	6	8
Elsinore (W+GI) Bilateral	17	0	10			
Elsinore (W+GI) N-S Rupture	17	0	17			
Elsinore (GI+T+J+CM) S-N Rupture	10	0	0			
Elsinore (GI+T+J+CM) N-S Rupture	10	0	168			

ACKNOWLEDGMENTS

The authors would like to thank the financial support they received that allowed them to conduct this investigation. The first author received funding from the John A. Blume fellowship and the Department of Civil and Environmental Engineering at Stanford University. The second author received funding from the National Agency for Research and Development (ANID) / Doctorado Becas Chile / 2019-72200307 from Chile, and from the Nancy Grant Chamberlain Fellowship from Stanford University. Partial funding for this research was also provided by the California Strong Motion Instrumentation Program of the California Geological Survey through agreement number 1023-003. The authors are grateful for this funding. The authors also thank the Southern California Earthquake Center (SCEC) for developing and providing access to the CyberShake study. This research would not have been possible without the availability of these valuable simulations. In particular, the authors would like to express gratitude to Scott Callaghan of SCEC for his guidance on accessing and downloading the CyberShake files.

DECLARATION OF CONFLICTING INTEREST

The authors declare no conflicts of interest with respect to the research, authorship, and/or publication of this article

REFERENCES

Aki K and Richards PG (2009) *Quantitative Seismology*. 2nd edition, corrected printing. Mill Valley, California New York: University Science Books.

Ancheta TD, Darragh RB, Stewart JP, et al. (2014) NGA-West2 Database. *Earthquake Spectra* 30(3). SAGE Publications Ltd STM: 989–1005.

ASCE, American Society of Civil Engineers (ed.) (2022) *Minimum Design Loads and Associated Criteria for Buildings and Other Structures: ASCE/SEI 7-22*. Reston: American Society of Civil Engineers.

Bijelić N, Lin T and Deierlein GG (2018) Validation of the SCEC Broadband Platform simulations for tall building risk assessments considering spectral shape and duration of the ground motion. *Earthquake Engineering & Structural Dynamics* 47(11): 2233–2251.

Boore DM (2010) Orientation-Independent, Nongeometric-Mean Measures of Seismic Intensity from Two Horizontal Components of Motion. *Bulletin of the Seismological Society of America* 100(4): 1830–1835.

Burks LS and Baker JW (2014) Validation of Ground-Motion Simulations through Simple Proxies for the Response of Engineered Systems. *Bulletin of the Seismological Society of America* 104(4): 1930–1946.

Burks LS, Zimmerman RB and Baker JW (2015) Evaluation of Hybrid Broadband Ground Motion Simulations for Response History Analysis and Design. *Earthquake Spectra* 31(3). SAGE Publications Ltd STM: 1691–1710.

Fayaz J, Azar S, Dabaghi M, et al. (2020) Methodology for Validation of Simulated Ground Motions for Seismic Response Assessment: Application to CyberShake Source-Based Ground Motions. *Bulletin of the Seismological Society of America* 111(1): 226–241.

Galasso C, Kaviani P, Tsioulou A, et al. (2020) Validation of Ground Motion Simulations for Historical Events using Skewed Bridges. *Journal of Earthquake Engineering* 24(10). Taylor & Francis: 1652–1674.

Girmay N, Poulos A and Miranda E (2023) Directionality and polarization of response spectral ordinates in the 2023 Kahramanmaras, Türkiye earthquake doublet. *Earthquake Spectra*. SAGE Publications Ltd STM. Epub ahead of print 19 October 2023. DOI: 10.1177/87552930231203989.

Girmay N, Miranda E and Poulos A (2024) Orientation and intensity of maximum response spectral ordinates during the December 20, 2022 Mw 6.4 Ferndale, California earthquake. *Soil Dynamics and Earthquake Engineering* 176: 108323.

Graves R, Jordan TH, Callaghan S, et al. (2011) CyberShake: A Physics-Based Seismic Hazard Model for Southern California. *Pure and Applied Geophysics* 168(3): 367–381.

Graves RW and Pitarka A (2010) Broadband Ground-Motion Simulation Using a Hybrid Approach. *Bulletin of the Seismological Society of America* 100(5A): 2095–2123.

Hong HP and Goda K (2007) Orientation-Dependent Ground-Motion Measure for Seismic-Hazard Assessment. *Bulletin of the Seismological Society of America* 97(5): 1525–1538.

Huang Y-N, Whittaker AS and Luco N (2008) Maximum Spectral Demands in the Near-Fault Region. *Earthquake Spectra* 24(1): 319–341.

Hull AG and Nicholson C (1992) Seismotectonics of the northern Elsinore fault zone, southern California. *Bulletin of the Seismological Society of America* 82(2): 800–818.

Magistrale H and Rockwell T (1996) The central and southern Elsinore fault zone, southern California. *Bulletin of the Seismological Society of America* 86(6): 1793–1803.

Mai PM, Imperatori W and Olsen KB (2010) Hybrid Broadband Ground-Motion Simulations: Combining Long-Period Deterministic Synthetics with High-Frequency Multiple S-to-S Backscattering. *Bulletin of the Seismological Society of America* 100(5A): 2124–2142.

NEHRP Consultants Joint Venture (2011) *Selecting and Scaling Earthquake Ground Motions for Performing Response-History Analysis,*. NIST GCR 11-917-15, Technical Report. Available at: https://www.nehrp.gov/pdf/nistgcr11-917-15.pdf (accessed 3 August 2023).

Poulos A and Miranda E (2022) Probabilistic characterization of the directionality of horizontal earthquake response spectra. *Earthquake Engineering & Structural Dynamics* 51(9): 2077–2090.

Poulos A and Miranda E (2023a) Effect of Style of Faulting on the Orientation of Maximum Horizontal Earthquake Response Spectra. *Bulletin of the Seismological Society of America* 113(5): 2092–2105.

Poulos A and Miranda E (2023b) Modification of Ground-Motion Models to Estimate Orientation-Dependent Horizontal Response Spectra in Strike-Slip Earthquakes. *Bulletin of the Seismological Society of America* 113(6): 2718–2729.

Poulos A and Miranda E (2024) Directionality characteristics of horizontal response spectra from the 2022 M_W 6.9 Chihshang, Taiwan earthquake. *Submitted to Earthquake Spectra*.

Shahi SK and Baker JW (2014) NGA-West2 Models for Ground Motion Directionality. *Earthquake Spectra* 30(3). SAGE Publications Ltd STM: 1285–1300.

Somerville PG, Smith NF, Graves RW, et al. (1997) Modification of Empirical Strong Ground Motion Attenuation Relations to Include the Amplitude and Duration Effects of Rupture Directivity. Seismological Research Letters 68(1): 199–222.

Teng G and Baker J (2019) Evaluation of SCEC CyberShake Ground Motions for Engineering Practice. *Earthquake Spectra* 35(3). SAGE Publications Ltd STM: 1311–1328.